

a very young embedded cluster of protostars near the Galactic Centre is thrown open here, although other explanations (a luminous evolved star such as an OH/IR star or a dust-enshrouded supergiant; Becklin et al., 1978, Rieke et al., 1978) have been considered in the past. Yet the fact that there are massive young stars such as WR stars and a cluster of HeI stars in the IRS16 complex near SgrA* (see the review of Genzel et al., 1995¹) begs the question whether massive star formation continues in the Galactic-Centre region, even though no compact radio sources or ultracompact HII regions have been found.

It would be particularly worthwhile to extend the current 10-micron search for massive protostars to the Galactic Centre circumnuclear disk of dense molecular gas (e.g. Genzel, 1989).

A 5 × 5 mosaic of 10-micron TIMMI images would cover most of the relevant area. This TIMMI project would benefit greatly from the successful implementation of the 3.6-m refurbishment plan (M2 mirror), as it would probably enable us to

¹In this review, Genzel et al. display a K-band spectrum of IRS3 obtained with their 3D spectrometer at the ESO-MPIA 2.2-m telescope. This spectrum shows a hint of weak HeI 2.06-micron emission on an otherwise featureless rising continuum, indicative of a highly reddened hot massive star. Krabbe et al. (1995) also mention that IRS3 could be a young massive star, although in their paper the HeI feature in IRS3 is barely discernible. Long ago, Rieke et al. (1978) already suspected that IRS3 could be a very young stellar object.

reach the 10-micron diffraction limit of 0.7 arcsec. This would much improve the 10-micron point source sensitivity and the chance of detecting massive protostellar objects in the circumnuclear ring. On the other hand, ISOCAM images may soon reveal the presence (or absence) of young stellar sources in the circumnuclear disk region, albeit with poorer spatial resolution. Follow-up diffraction-limited imaging with TIMMI is likely to be needed. We hope for the best possible image quality at the 3.6-m by then.

Finally, we briefly discuss our results on IRS7 and SgrA* (which are in agreement with those of Gezari et al., 1994a,b). IRS7 – the brightest source in the 2.2-micron K-band – is not detected in our images, suggesting that this red supergiant lacks a warm optically thick dust shell. However, IRS7 is clearly detected at 7.8 and 12.4 micron (see Gezari et al., 1994a), suggesting that our non-detection at 10.1 microns may be due to absorption in the silicon feature around 9.7 microns, either locally or along the line of sight. As for SgrA*, we see no mid-infrared source at its position, which may imply that there is no or very little warm dust in the immediate vicinity of the Galactic-Centre monster. However, SgrA* has been claimed to be detected in deep 8.7-micron images (S. Stolovy, data presented at the recent ESO/CTIO conference in La Serena).

P.S. We have also obtained 10.4-micron [Si V] and 12.8-micron [Ne II] narrow-band images of the innermost

Galactic-Centre region, in an attempt to study the spatial distribution of the energy and excitation sources in this region.

References

- Becklin, E. et al., 1978, *ApJ* **219**, 121.
 Genzel, R., 1989, IAU Symp 136 (ed. M. Morris).
 Genzel, R., Eckart, A., Krabbe, A., 1995, *Ann. N.Y. Acad. Sci.* **759**, 38 (eds. Böhringer, H., Morfill, G.E., Trümper, J. (Proc. 17th Texas Symposium Munich)).
 Gezari, D. et al., 1985, *ApJ* **299**, 1007.
 Gezari, D. et al., 1994a, in: *The Nuclei of Normal Galaxies: Lessons from the Galactic Center*, eds. R. Genzel and A. Harrig, Kluwer, p. 343.
 Gezari, D. et al., 1994b, *ibidem*, p. 427.
 Herbst, T.M., Beckwith, S.V.W., Shure, M., 1993, *ApJ* **411**, L21.
 Jackson, J.M. et al., 1993, *ApJ* **402**, 173.
 Käuffl, H.U. et al., 1992, *The Messenger* **70**, 67.
 Käuffl, H.U. et al., 1994, *Infrared Phys. Technol.* **33**, 203.
 Käuffl, H.U. 1995, in *ESO/ST-ECF Workshop on Calibration and Understanding HST and ESO Instruments*, ed. P. Benvenuti, p. 99.
 Krabbe, A., et al. 1995, *ApJ* **447**, L95.
 Rieke, G. et al., 1978, *ApJ* **220**, 556.
 Rieke, G., Lebofsky, M., 1985, *ApJ* **288**, 616. (Tab. 3).
 Wynn-Williams, G. et al. (1984). *ApJ* **281**, 172.

Hans Zinnecker
 e-mail: hzinnecker@aip.de

Redshift and Photometric Survey of the X-Ray Cluster of Galaxies Abell 85

F. DURRET^{1, 2}, P. FELENBOK², D. GERBAL², J. GUIBERT³, C. LOBO^{1, 4} and E. SLEZAK⁵

¹Institut d'Astrophysique de Paris; ²DAEC, Observatoire de Paris-Meudon; ³CAI, Observatoire de Paris; ⁴CAUP, Porto; ⁵O.C.A., Nice

As the largest gravitationally bound systems in the Universe, clusters of galaxies have attracted much interest since the pioneering works of Zwicky, who evidenced the existence of dark matter in these objects, and later of Abell, who achieved the first large catalogue of clusters.

Clusters of galaxies are now analysed through three different and complementary approaches: optical imaging and spectroscopy, which allow to derive the galaxy content, X-ray imaging and spectroscopy, giving information on the physical properties of the X-ray gas embedded in the cluster, and from which the total dynamical mass of the cluster can be estimated, under the assumption of

hydrostatic equilibrium, and, for clusters of redshifts $z \geq 0.31$ deep optical imaging of arcs and arclets in clusters.

As a complementary approach to that of large cluster surveys such as the ENACS (ESO Nearby Abell Cluster Survey) ESO key programme, we have chosen to analyse in detail a few clusters of galaxies, by combining optical and X-ray data. We present here results on the first of the two clusters observed at ESO: Abell 85.

This cluster is rich and located at a redshift $z \sim 0.055$, corresponding to a spatial scale of 97.0 kpc/arcmin ($H_0 = 50$ km/s/Mpc). Previously published data on this cluster include partial CCD imaging by Murphy (1984), redshift catalogues by

Beers et al. (1991) and Malumuth et al. (1992), totalling 150 redshifts; these authors evidenced the existence of substructure in Abell 85 as well as the presence of a foreground group of galaxies. Abell 85 has a double structure in X-rays (Gerbai et al., 1992 and references therein), and is therefore not fully relaxed, as many other clusters indeed, contrarily to what was previously believed.

Observations

We first obtained a photometric catalogue of 4232 galaxies (hereafter the MAMA catalogue) in a region of $\pm 1^\circ$ around the cluster centre, by scanning a b_j photographic plate with the MAMA

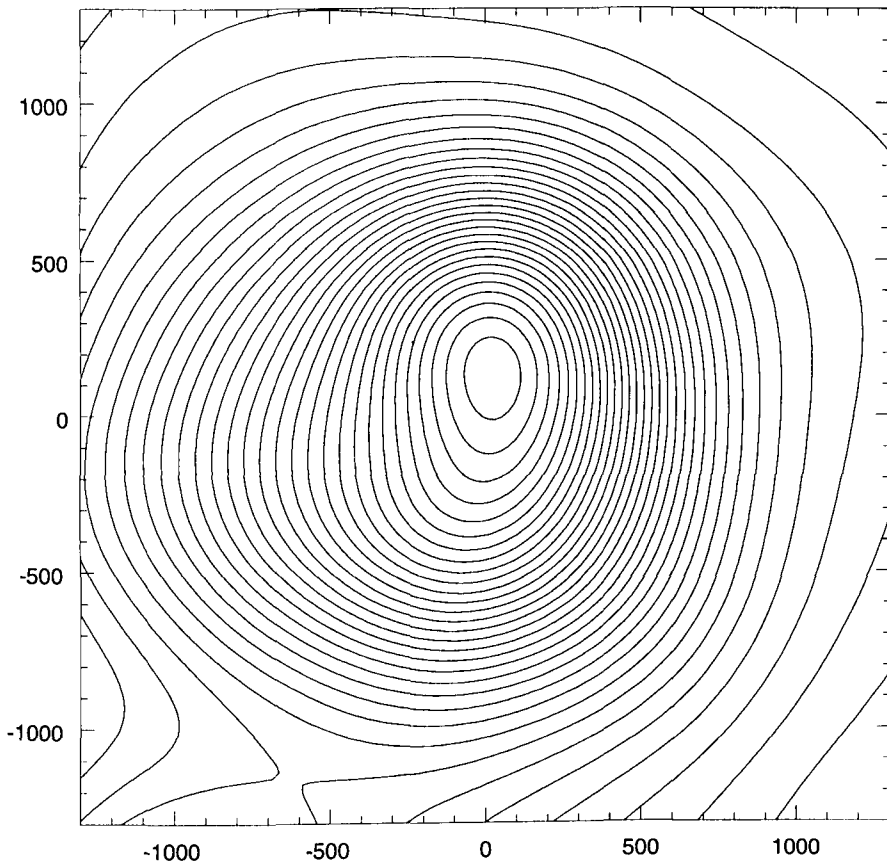


Figure 1. Kernel map distribution of the galaxies in the central regions of the MAMA photometric catalogue of Abell 85 (as defined in text), obtained with 10 bootstrap resamplings. Co-ordinates are in arcseconds relative to the centre.

measuring machine at the CAI, Observatoire de Paris. This catalogue is complete for $b_j \leq 18.0$; the galaxy positions obtained are very accurate (1–2") while magnitudes are not due to usual problems with photographic plates.

We therefore made observations of six fields of $6.4 \times 6.4'$ in the central regions of the cluster with the Danish 1.5-m telescope in the V and R bands. Reductions were made with IRAF and using the software developed by O. Le Fèvre. This allowed us to recalibrate the magnitudes of our MAMA catalogue, and also to obtain a deeper photometric catalogue in V and R of the central regions of the cluster (hereafter the CCD catalogue).

Spectroscopic observations were performed with the ESO 3.6-m telescope equipped with MEFOS, and a dispersion of 224 Å/mm in the wavelength region 3820–6100 Å, during 6 and 2 nights in November 1994 and 1995. We obtained 421 reliable redshifts, leading to a spectroscopic catalogue of 592 objects in this region, 551 of them being galaxies (including the 150 published by Beers et al., 1991 and Malumuth et al., 1992). The reduction was made with IRAF and velocities were measured using cross-correlation techniques.

Projected Galaxy Distribution

We performed a kernel analysis of the MAMA photometric catalogue described

above and display the result in Figure 1. The main structure of the cluster appears very smooth, with a clear elongation towards the south in the central region coinciding with the presence of the South blob observed in X-rays (see Gerbal et al., 1992). This confirms the idea that Abell 85 is bimodal, with a main body in which both the galaxies and the hot intracluster gas appear smoothly distributed, and a blob south of the central zone.

Velocity Distribution

The velocity distribution of the 551 galaxies of our redshift catalogue is displayed in Figure 2 as a function of distance to the cluster centre. We can see from this figure that there is indeed a "sheet" of galaxies with velocities of about 6000 km/s, as mentioned by previous authors. Behind the cluster, there is a large number of galaxies following a velocity distribution suggestive of a certain periodicity that could correspond to voids and sheets of galaxies and could therefore be used as an indicator of large-scale structures in this direction.

A good agreement between the mean and median values of the velocities is

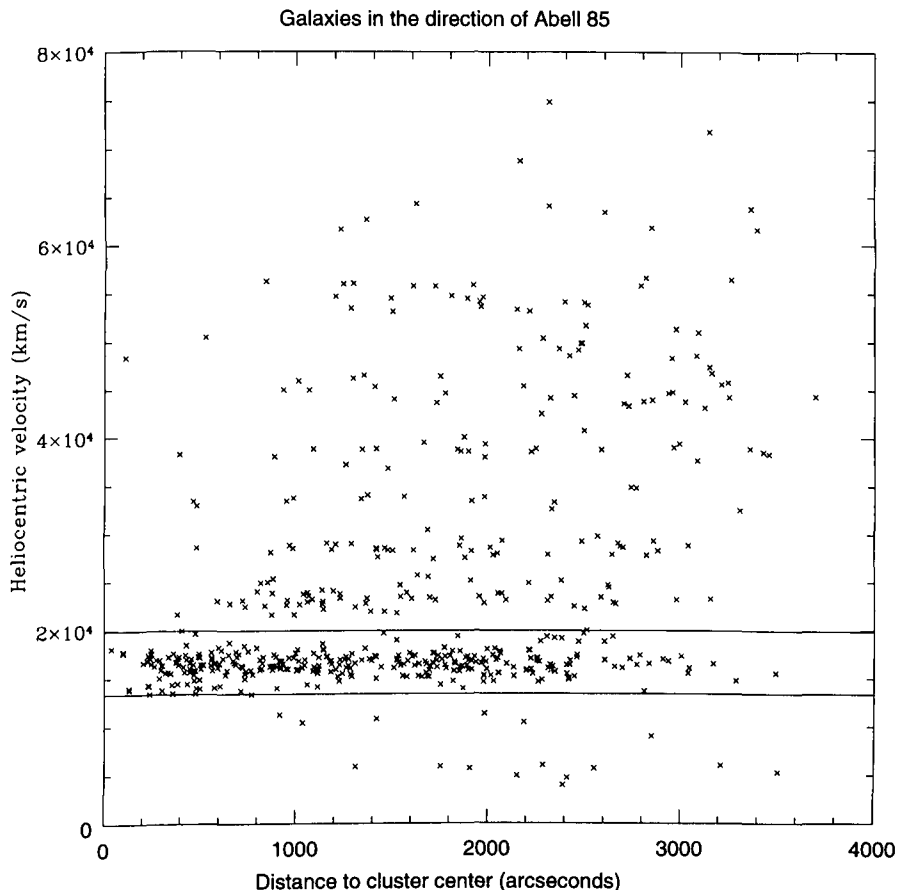


Figure 2. Velocity distribution as a function of distance to the cluster centre, with two lines indicating the velocity range in the cluster.

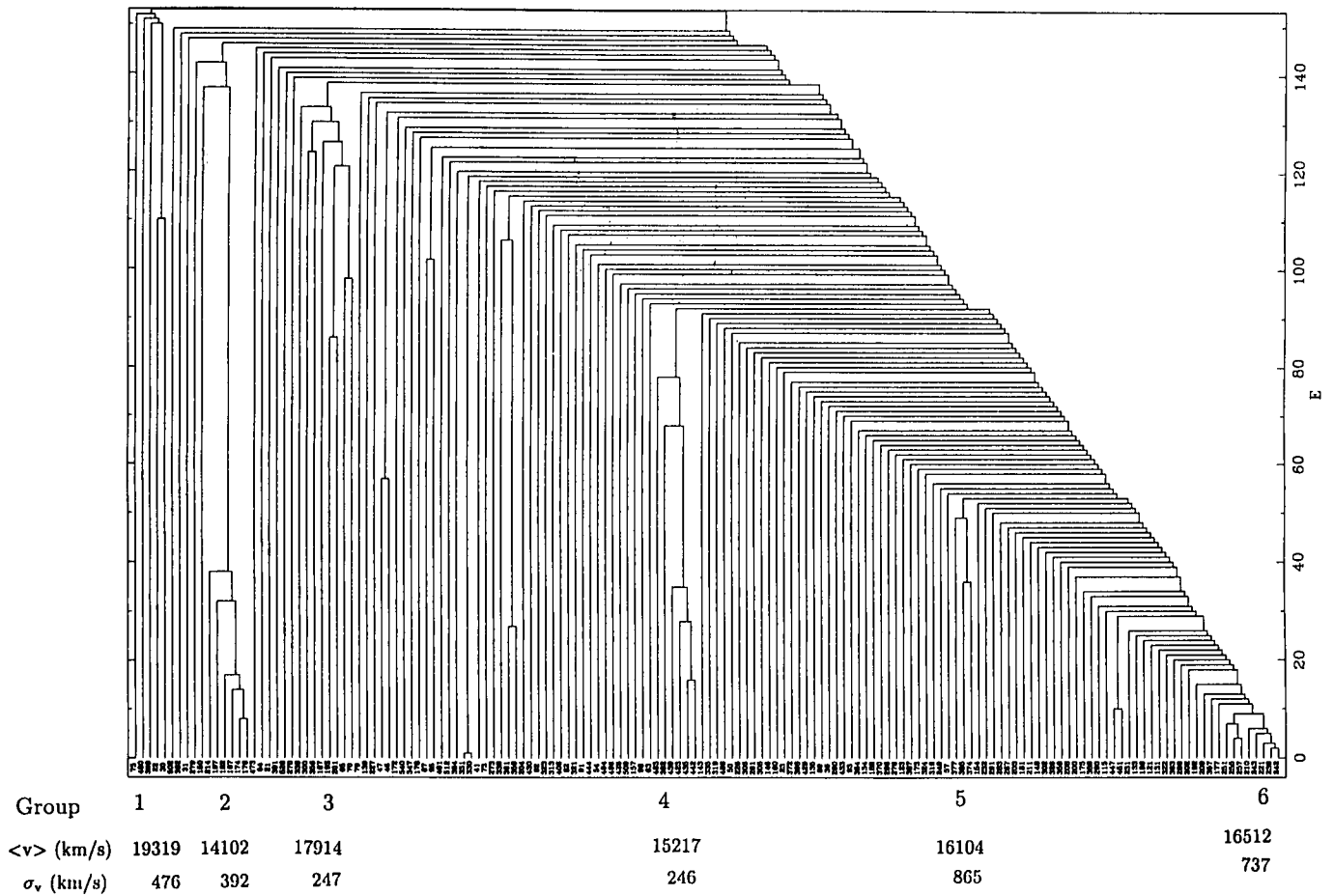


Figure 3. Result of the hierarchical test performed on the 154 brightest members of Abell 85, where E represents the binding energy of the system and the tiny numbers are the catalogue numbers for each galaxy. From left to right, groups 1 to 6 are indicated below the figure, as well as the average velocity and velocity dispersion of each group.

obtained in the interval $13,350 \leq v \leq 19,930$ km/s, which will be taken as the criterion for galaxies to belong to Abell 85. This leads to a total number of 308 galaxies with measured velocities belonging to Abell 85, making this velocity catalogue (hereafter the A 85 velocity catalogue) one of the richest ones for a single cluster.

The bi-weight mean velocity for this sample is 16,458 km/s, with a high velocity dispersion of 1185 km/s, in agreement with the existence of substructure.

The velocity of the cD galaxy is $16,734 \pm 48$ km/s and $16,447 \pm 126$ km/s as given by Beers et al. (1991) and Malumuth et al. (1992) respectively. We will use the Beers et al. value, which has the smallest error bar; this value is equal to the mean cluster velocity within error bars.

Search for Clustering Patterns

In order to search for substructure in Abell 85, we have performed on the A 85 velocity catalogue a hierarchical test based on the binding gravitational energy of galaxies (see Serna & Gerbal, 1996 for a full description of the method).

The result of such an analysis is displayed and reveals several interesting features. From left to right on Figure 3:

Groups 1 and 3 are probably just isolated background galaxies (their spatial distribution shows no concentration), while Group 2 has a velocity close to the lower limit of that of the cluster and appears tight in projection. All the other

galaxies can be considered to form the actual Abell 85 cluster, for which the velocity dispersion then becomes 760 km/s, a value more typical of rich clusters than the high value given above when analysing the whole A 85 velocity cata-

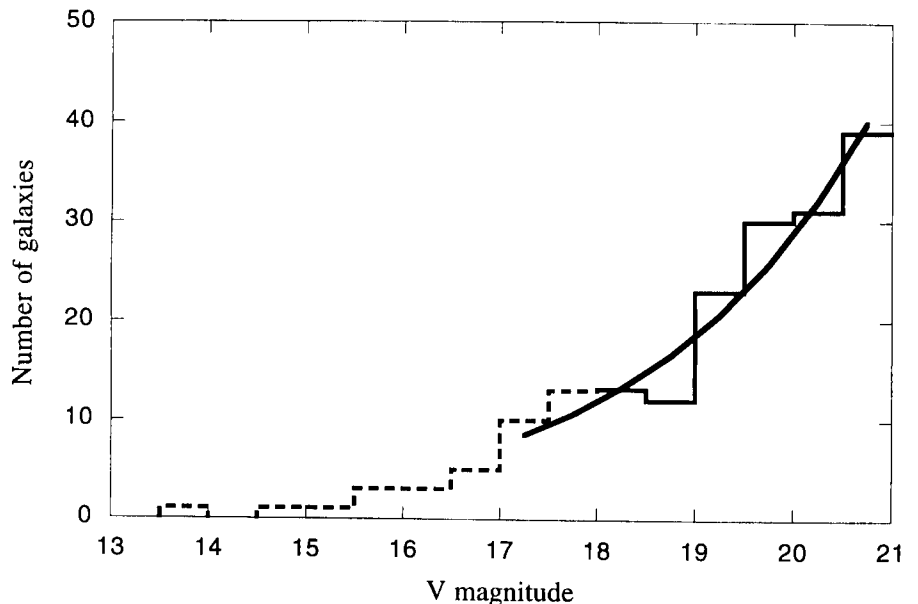


Figure 4. Luminosity function in the V band for the CCD catalogue (defined in text) and best fit with a power law of index $\alpha = -1.5 \pm 0.1$.

logue. Group 4 includes 6 galaxies close in projection (in particular 4 of them), Group 5 is a triplet very close in projection, and Group 6 is located at the bottom of the potential well, around the cD galaxy.

Luminosity Function in the V Band

The luminosity function in the V band shown in Figure 4 has been derived:

- directly, for the brightest galaxies ($V < 18$) with velocities belonging to the cluster;

- for fainter galaxies, for all the objects of our CCD photometric catalogue, to which we have subtracted the background counts in the V band taken from the ESO-Sculptor survey (Bellanger et al., 1995, Arnouts et al., 1996, see preprint by Lobo et al., 1996 for details on this subtraction).

The best fit is obtained for a power law of index $\alpha = -1.5 \pm 0.1$, similar to that obtained in central regions of clusters, such as e.g. in Coma, which we have

re-analysed in detail recently (Biviano et al., 1996, Lobo et al., 1996 and references therein).

Conclusions

The combined data obtained with the MAMA measuring machine, CCD imaging and spectroscopy with MEFOS have led to one of the richest velocity catalogues for a single cluster. This will allow a detailed analysis of the physical properties of Abell 85, which will be compared to those derived from X-rays (Pislar et al., 1996).

Acknowledgements

We gratefully acknowledge A. Biviano for supplying us with his adaptive kernel programme, O. Le Fèvre for giving us his photometric analysis software, and A. Serna for giving us his hierarchical test programme.

CL is fully supported by the BD/2772/93RM grant attributed by JNICT, Portugal.

References

- Arnouts S., de Lapparent V., Mathez G. et al. 1996, *A&AS* in press.
- Beers T.C., Forman W., Huchra J.P., Jones C., Gebhardt K. 1991, *AJ* **102**, 1581.
- Bellanger C., de Lapparent V., Arnouts S., et al. 1995, *A&AS* **110**, 159.
- Biviano A., Durret F., Gerbal D., Le Fèvre O., Lobo C., Mazure A., Slezak E. 1996, *A&A* in press.
- Gerbal D., Durret F., Lima-Neto G., Lachièze-Rey M. 1992, *A&A* **253**, 77.
- Lobo C., Biviano A., Durret F., Gerbal D., Le Fèvre O., Mazure A., Slezak E. 1996, *A&A* submitted.
- Malumuth E.M., Kriss G.A., Van Dyke Dixon W., Ferguson H.C., Ritchie C. 1992, *AJ* **104**, 495.
- Murphy P. 1984, *MNRAS* **211**, 637.
- Pislar V., Durret F., Gerbal D., Lima-Neto G., Slezak E., 1996, to be submitted to *A&A*.
- Serna A., Gerbal D. 1996, *A&A* in press.
- Slezak E., Durret F., Gerbal D. 1994, *AJ* **108**, 1996.

Florence Durret
e-mail: durret@iap.fr

Fishing for Absorption Lines with SEST

THE REDSHIFT OF THE GRAVITATIONAL LENS TO PKS 1830–211

T. WIKLIND (*Onsala Space Observatory, Sweden*)

F. COMBES (*DEMIRM, Observatoire de Paris, France*)

Background

Molecular gas is the cold and dense part of the interstellar medium (ISM) which is directly involved in the formation of stars. The possibility of studying this ISM component at high redshifts would give us an insight in the conditions for stellar formation when these may have been quite different from what is seen in present-day galaxies. It was therefore with great interest that astronomers greeted the news in 1991 that emission from the rotational $J=3-2$ line of carbon monoxide (CO) had been detected in the galaxy F10214+4724 at a redshift of $z = 2.29$ (Brown & Vanden Bout, 1991). A standard conversion factor between the integrated CO emission and the column density of H_2 implied a molecular gas mass of $2 \times 10^{11} M_\odot$, which meant that the molecular gas constituted a major part of the total mass of the galaxy. Three years later CO emission was detected in the Cloverleaf quasar at $z = 2.56$ (Barvainis et al., 1994). In this case it was known that the CO emission was magnified by gravitational lensing, making it impossible to derive the intrinsic H_2 mass. It is now clear that also F10214+4724 is a gravitationally lensed system (Matthews et al., 1994) and that the molecular gas mass is overestimated

by a factor of 10 or more (Radford, 1996). Yet another gravitationally lensed galaxy has been detected by Casoli et al. (1996). They observed CO emission from a gravitational arc at $z \approx 0.7$. With a magnification factor of ~ 50 , this is intrinsically a relatively inconspicuous galaxy.

Apart from these gravitationally lensed objects, there have been searches for CO emission in nonlensed systems at high redshifts, which have all been negative. In fact, there are no confirmed observations of CO emission in nongravitationally lensed objects at redshifts higher than $z \approx 0.3$. Hence, high- z galaxies, including those with detected CO emission, appear not to contain extremely high molecular gas masses. At most, they are similar to nearby examples of merger systems, such as Arp 220. Nevertheless, the lensed systems have shown that molecular gas which has undergone a substantial stellar processing does exist at high redshifts.

Gravitationally magnified CO emission is, however, not our only means to study molecular gas at high redshifts. Just as in the optical wavelength band, it is easier to detect molecular absorption lines than the corresponding emission lines and, with an appropriate alignment of an intervening galaxy and a background radio continuum source, it is

possible to probe the molecular ISM at very large distances. This has been demonstrated by the detection of more than 40 different molecular transitions at redshifts ranging from $z = 0.25$ to $z = 0.89$ (Wiklind & Combes, 1994, 1995a, 1995b; Combes & Wiklind, 1995). Due to the greater sensitivity of absorption lines, it is possible to observe molecules other than CO. Paradoxically, this is easier to do for gas at large distances, since Galactic absorption almost always gets confused with emission.

Molecular Absorption Lines at Intermediate Redshifts

The first molecular absorption at a cosmologically significant distance was detected with the SEST telescope in December 1993, towards the BL Lac object PKS1413+135 (Wiklind & Combes, 1994). The CO($J = 1 \leftarrow 0$) transition was seen at a redshift of $z = 0.247$. The continuum radio source is completely obscured at optical wavelengths and coincides with an edge-on galaxy with the same redshift as the absorption. The redshift of the BL Lac itself is not known, but since the impact parameter between the radio core and the nucleus of the galaxy is $< 0.1''$ and since there are no indications of gravitational lensing effects, it